SciMedCentral

JSM Biotechnology & Biomedical Engineering

Short Communication

Novel Biocompatible Cobalt Oxide Nanoparticles for Use in Dual Photoacoustic and Magnetic Resonance Imaging

Yu Kimura[1,2], Takuya Kurimoto[2], Yuta Imai[2] Hiro-aki Sugii[2], Akio Toshimitsu[2,3], Tetsuya Matsuda[4], Hirohiko Imai[4], Hisatsugu Yamada[2,5] and Teruyuki Kondo[2,5]*

[1]*Research and Educational Unit of Leaders for Integrated Medical System, Center for the Promotion of Interdisciplinary Education and Research, Kyoto University, Japan*
[2]*Department of Energy and Hydrocarbon Chemistry, Graduate School of Engineering, Kyoto University, Japan*
[3]*Division of Multidisciplinary Chemistry, Institute for Chemical Research, Kyoto University, Japan*
[4]*Department of Systems Science, Graduate School of Informatics, Kyoto University, Japan*
[5]*Advanced Biomedical Engineering Research Unit, Center for the Promotion of Interdisciplinary Education and Research, Kyoto University, Japan*

***Corresponding author**
Teruyuki Kondo, Advanced Biomedical Engineering Research Unit, Center for the Promotion of Interdisciplinary Education and Research, Kyoto University, Katsura, Nishikyo-ku, Kyoto 615-8510, Japan, Tel: 81-75-383-7055; Fax: 81-75-383-2805; E-mail: teruyuki@scl.kyoto-u.ac.jp

Submitted: 30 October 2014
Accepted: 03 November 2014
Published: 05 November 2014
ISSN: 2333-7117

Keywords
- Nanoparticle
- Cobalt oxide
- Imaging probe
- Photoacoustic imaging
- Magnetic resonance imaging

Abstract

Novel biocompatible poly(ethylene glycol) (PEG)-stabilized CoO nanoparticles have been synthesized. The particles exhibited a near-infrared laser-based photoacoustic signal that was 11 times stronger than that of our previously developed gadolinium oxide nanoparticles. The value of r_2/r_1 determined by 7 T MRI at room temperature was similar to that of a clinically-used negative MRI contrast agent, Resovist®. These results indicate that the present PEG-stabilized CoO nanoparticles may be highly effective as a bimodal contrast agent for photoacoustic and magnetic resonance imaging.

ABBREVIATIONS

PAT: Photoacoustic Tomography; **MRI:** Magnetic Resonance Imaging

INTRODUCTION

The imaging and diagnosis of diseases, especially of cancers, have increased in importance with respect to improving patients' quality of life through the much earlier detection of abnormalities and monitoring following treatment. To achieve these goals, many diagnostic modalities, including magnetic resonance imaging (MRI), positron emission tomography (PET) and single photon emission computed tomography (SPECT), have been vigorously developed [1]. In addition, multimodal imaging techniques that combine several modalities have recently been the subject of research to overcome the drawbacks of each modality by itself, such as limitations in sensitivity or acquisition depth [2,3]. We previously synthesized biocompatible gelatin-coated gadolinium oxide (Gd_2O_3) nanoparticles without requiring gold nanorods or dyes, which are effective as dual photoacoustic (PA) and magnetic resonance (MR) imaging probes [4]. PA imaging, also known as laser optoacoustic imaging, is as an emerging noninvasive, nonionizing, and deeply penetrating imaging modality [5,6] which combines the sensitivity of optical methods with the resolution of diffraction-limited ultrasound. For the PA imaging of tumors, blood vessels, hemoglobin oxygenation, and tumor angiogenesis, gold nanoshells [7], nanocages [8,9], nanorods [10-15], and nanobeacons [16] have generally been used as contrast agents. To date, however, there have been no reports on either a mechanism for the elimination of gold from the body or the detailed toxicity of gold.

Cobalt is an essential element in our bodies where it is part of a coenzyme called coballamine [17]. Cobalt complexes with various valence conditions give a variety of colors, which is caused by the d-d transition of electrons. Therefore, these compounds would be good candidates for photoacoustic agents because of their light absorption properties. Moreover, cobalt has $3d^7$ electrons which are suitable for magnetic resonance imaging and has already been used as a positive contrast agent for magnetic resonance imaging (MRI) [18], in which gold metal nanocomposites were used as a dual MRI and PA imaging probe. In the present study,

we synthesized water-dispersible cobalt oxide nanoparticles stabilized with PEG, and evaluated their suitability for use as dual PA and MR imaging probes that do not require conjugation with gold, rare earth metals, or dyes.

MATERIALS AND METHODS

Materials

Cobalt(III) acetylacetonate ($Co(acac)_3$, 97%, Nacalai Tesque, Kyoto, Japan), ethanol (99.5%, Nacalai Tesque), poly(ethylene glycol) (PEG; Mw: 2,000, Wako Chemical Industry, Osaka, Japan), and chloroform (99%, Nacalai Tesque) were obtained commercially and used without further purification. Oleylamine (Tokyo Chemical Industry Co. Ltd, Tokyo, Japan) was distilled before the experiment. Ultra-pure water was prepared by a Millipore Direct-Q 3UV system (Millipore Inc., Billerica, MA).

The concentration of Co was determined by atomic absorption spectrometry using a cobalt standard solution (100 ppm, Nacalai Tesque) that was prepared before the experiment. Resovist® (ferucarbotran, Fujifilm RI Pharma Ltd., Tokyo, Japan) was chosen as a comparison to evaluate the novel cobalt oxide nanoparticles by MRI.

Synthesis of water-dispersible cobalt oxide nanoparticles

Cobalt(III) acetylacetonate (83 mg, 0.23 mmol) was dissolved with oleylamine (15.4 mL, 47 mmol) at 135 °C under an Ar atmosphere and heated with a microwave reactor (Initiator Eight, Biotage, Uppsala, Sweden) at 200 °C for 1 hr. The homogeneous green mixture was cooled to room temperature, and then dropped into ethanol (40 mL), which led to the precipitation of cobalt oxide nanoparticles covered with oleylamine. Cobalt oxide nanoparticles were isolated by centrifugation (6,400 g × 10 min) and the precipitate was washed with ethanol (40 mL × 3). After the isolated cobalt oxide nanoparticles were dispersed into chloroform (4.0 mL), PEG (20 mg, 0.010 mmol) was added and the mixture was stirred for 15 hr. After chloroform was evaporated, PEG-stabilized cobalt oxide nanoparticles were obtained, and they could be dispersed into ultra-pure water without aggregation.

Characterization

The hydrodynamic mean diameter of nanoparticles dispersed in ultra-pure water was determined by dynamic light scattering analysis (DLS, Zetasizer Nano NS, Malvern Instruments, Worcestershire, UK). The surface electric potential of nanoparticles, which is called the zeta potential, was determined by electrophoresis light scattering analysis (ELS, Zetasizer Nano NS). Transmission electron microscopic (TEM) images of the nanoparticles were obtained with JEM-1400 microscope (JEOL Ltd. Tokyo, Japan). The nanoparticles dispersed in water were dropped onto a carbon-spattered Cu grid, and the grid was air-dried. The ratio and concentration of Co in the nanoparticles were determined by thermogravimetry-differential thermal analysis (TG-DTA, TG8120, Rigaku Co. Tokyo, Japan) and atomic absorption spectrometry (AAS, Z-2710, Hitachi Ltd. Tokyo, Japan). For TG-DTA analysis, the temperature of the sample was increased to 1000 °C at a rate of 10 °C/min under an air-flow of 50 cm^3/min.

For measurements and evaluation of the longitudinal and transverse relaxation times (T_1 and T_2) by MRI, dispersions of synthesized cobalt oxide nanoparticles in ultra-pure water were prepared at 1.0, 0.50, 0.25 and 0.10 mM, while the concentrations of ferucarbotran were adjusted to 1.0, 0.50, 0.25 and 0.10 mM. MR images and longitudinal and transverse relaxation times were obtained and measured by a 7T MRI instrument for small animals at 25 °C (BioSpec 7.0T/20 USR with a 72 mm i.d. Quadrature resonator, Bruker Biospin, Ettlingen, Germany). T_1 was obtained by fast imaging with steady state (FISP) with an inversion pulse (inversion time = 65 - 5729 ms, repetition time (TR) = 3 ms, echo time (TE) = 1.5 ms, field of view (FOV) = 4 × 4 cm^2, matrix size = 128 × 128, thickness of slice = 2 mm, and number of data accumulations (NA) = 2). T_2 was measured by a multiecho spin-echo (SE) sequence with a flipback pulse (TE = 10 - 320 ms, TR = 2000 ms, FOV = 4 × 4 cm^2, matrix size = 128 × 128, slice thickness = 2 mm, and NA = 1). Longitudinal and transverse relaxivity indices (r_1 and r_2, $Lmmol^{-1}s^{-1}$) were determined from the linear slope in concentration vs. $(1/T_i)$-$(1/T_i$ (solvent)) (longitudinal, i = 1; transverse, i = 2) graphs of the synthesized cobalt oxide nanoparticles and ferucarbotran.

In vivo experiment

All animal experiments were performed according to the Institutional Guidance of Kyoto University on Animal Experimentation and under the approval of the animal experiment committee of the Faculty of Engineering, Kyoto University. Mice (Balb/c, female) were anesthetized with 1-2% isoflurane (Forane®, Abbott Japan Ltd., Osaka, Japan). PA images were obtained immediately after subcutaneous injection of the synthesized cobalt oxide nanoparticles (0.059 mmol Co/kg) by a preclinical photoacoustic computed tomography scanner (Nexus 128, Endra Inc., Ann Arbor, MI) with the following conditions: laser intensity: 2.1 mJ at 37 °C, laser wavelength: 710 nm, ROI size: 20 × 20 mm^2, accumulation: 20 times, observation angle: 120°, z-axis resolution: 0.3 mm.

RESULTS AND DISCUSSION

Cobalt oxide nanoparticles in organic solvent were synthesized by the method described in a previous report, with some modification [19]. Isolated nanoparticles were mixed with PEG (Mw: 2,000) to stabilize the particles in water. PEG is easily hydrated and soluble in most of solvents, and is widely known to be a biocompatible molecule for the control of drug solubility and *in vivo* biodistribution [20]. In this experiment, PEG should also protect nanoparticles in water.

The composition of the nanoparticles was determined by X-ray diffractometry (XRD) and thermogravimetry-differential thermal analysis (TG-DTA). The XRD pattern indicated that the synthesized nanoparticles were composed of hexagonal CoO pyramids [21,22]. After the addition of PEG, the XRD pattern showed a merger of PEG and hexagonal CoO [23] (Figure 1a). TG-DTA indicated that synthesized nanoparticles were composed of 26.7 % inorganic metal oxides and 73.3 % organic materials like oleylamine and PEG. Transmission electron microscopy revealed that the CoO particle itself had a size of around 80 nm and a pyramidal shape (Figure 1b). In contrast, the mean diameter of particles in water was 191.3 nm, as determined by dynamic light

scattering (DLS) measurement, and this value did not change even after incubation at room temperature for 5 days (Figure 1c). Therefore, the CoO particles in water were thought to have been slightly aggregated and stabilized by the protective effects of PEG [24]. Based on the zeta potential, the surface potential of PEG-stabilized CoO nanoparticles was +32.1 mV. This value is likely due to surface oleylamine molecules in a PEG-protected layer. This electrostatic repulsion as well as the hydration effect with PEG should affect the stability of CoO nanoparticles in water.

A UV-Visible absorption spectrum was obtained for the water suspension of CoO nanoparticles. As a result, the synthesized nanoparticles gave an absorption peak at 680 nm (data not shown) and the molar coefficient at 710 nm was 1.86×10^9 (mol particle · $L^{-1}cm^{-1}$). This value is 36 times higher than that of the previous Gd_2O_3 nanoparticles (5.15×10^7 mol particle. $L^{-1}cm^{-1}$). Indeed, the PA signal detected after irradiation of a water suspension of CoO nanoparticles with a pulsed laser was 11 times stronger (20.75 VM^{-1}) than that for a Gd_2O_3 nanoparticle suspension (1.81 VM^{-1}). This difference could be due to the much greater light absorption by CoO nanoparticles. It is widely known that the intensity of a PA signal strongly depends on the output of the pulsed laser, the adsorption coefficient of the nanoparticles, and the rate of conversion from light energy to thermal energy, as well as the Grünizen constant [14]. The Grünizen constant is comprised of the isobaric volume expansion coefficient, the isothermal compressibility, the density of the components, and the isochoric specific heat. Organic components generally have a higher expansion coefficient and a lower heat capacity than water. Therefore, the combination of metal oxide and organic components could contribute to the increase in the Grünizen constant of the particles, and to the subsequent increase in PA signal intensity.

In vivo PA images were obtained by a preclinical photoacoustic computed tomography (PAT) scanner. (Figure 2a) shows a PA image of the back of a mouse before and after subcutaneous injection of the synthesized CoO nanoparticles. After injection, an intense signal was observed at the injection site, even though the amount of metal is only 20% of that in Gd_2O_3 nanoparticles. T_2-weighted MR images (7T, r.t.) of solutions of synthesized nanoparticles and ferucarbotran and Co^{2+} are shown in Figure 2b. The MR imaging study showed that the synthesized CoO nanoparticles can shorten T_2 and darken the image than water (Figure 2b), and the r_2/r_1 value is similar to that of clinically available ferucarbotran (Resovist®) as a negative contrast agent (Table 1). The results indicated that the synthesized CoO nanoparticles were effective for use in dual PA and MR imaging.

CONCLUSION

We successfully developed new biocompatible PEG-stabilized

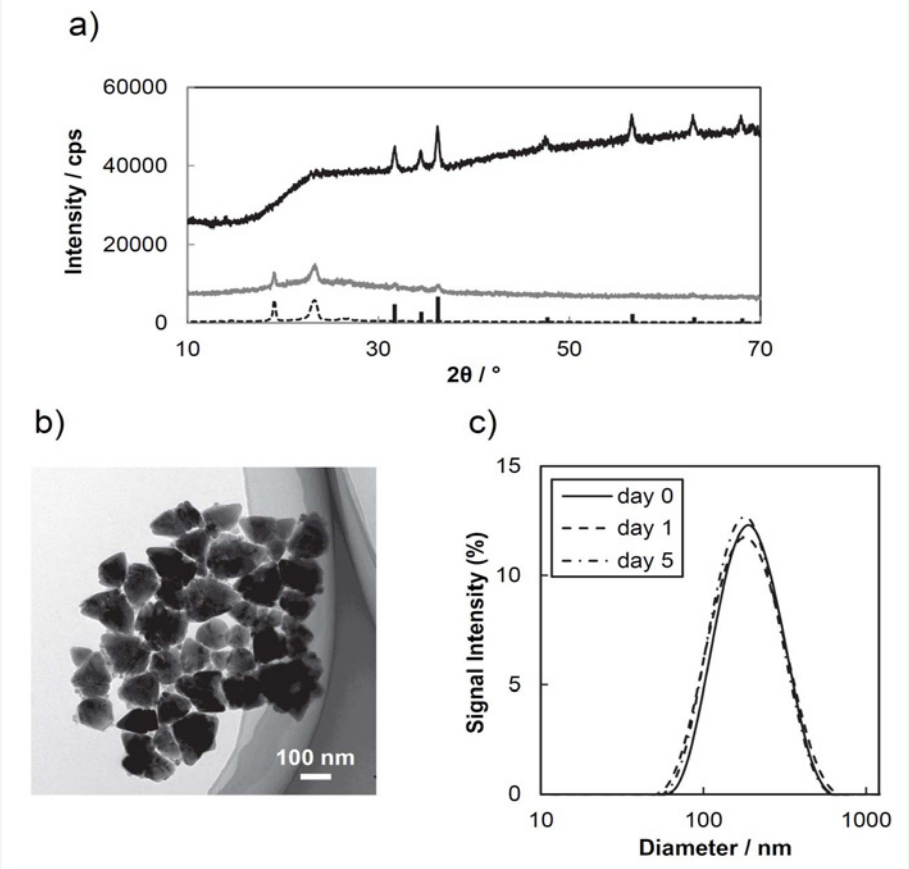

Figure 1 (a)– XRD pattern of synthesized cobalt oxide nanoparticles (upper; black), PEG-stabilized cobalt oxide nanoparticles (middle; gray) and PEG (lower; dashed). The vertical bars indicate XRD pattern of hexagonal CoO standards. (b) –Transmission electron microscopy of synthesized PEG-stabilized CoO nanoparticles. (c)– Dynamic light scattering of a water dispersion of synthesized nanoparticles.

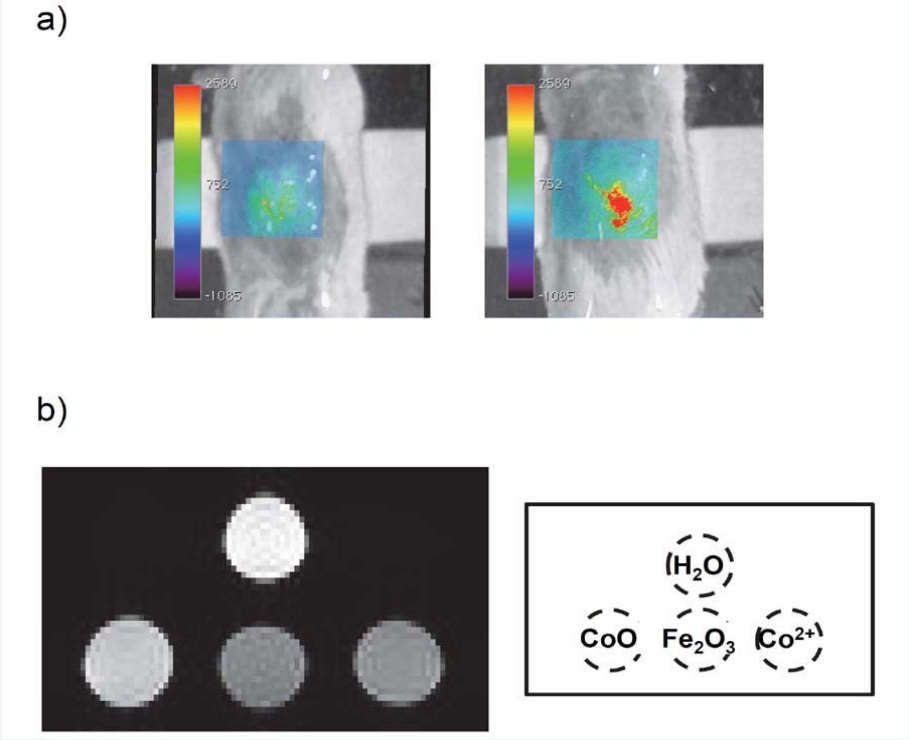

Figure 2 (a) – Photoacoustic tomography before and after subcutaneous injection of synthesized PEG-stabilized CoO nanoparticles. (b) $-T_2$-weighted magnetic resonance image of synthesized PEG-stabilized CoO nanoparticles, ferucarbotran (Resovist®; Fe_2O_3), Co^{2+} ($CoCl_2{\cdot}6H_2O$) (0.10 mM), and water.

Table 1: Longitudinal (r_1) and transverse (r_2) relaxivity of water proton in a suspension of synthesized PEG-stabilized CoO nanoparticles, ferucarbotran (Resovist®) and Co^{2+} ($CoCl_2{\cdot}6H_2O$).

	r_1 ($mM^{-1}s^{-1}$)	r_2 ($mM^{-1}s^{-1}$)	r_2/r_1
CoO nanoparticle	0.4	11.3	28.3
Resovist®	5.9	145	24.6
$CoCl_2{\cdot}6H_2O$	47	270	5.7

CoO nanoparticles, which enabled the synergistic coupling of PA and MR imaging. PAT in this study has a z –axis resolution of 0.3 mm, in contrast to the slice thickness of 2 mm in MRI. Thus, the combination of these two imaging modalities should improve the three-dimensional detection of a lesion *in vivo*. In addition, the combination of both imaging modalities may be useful for the coarse detection of diseases in the whole body with MRI, while more precise information could be obtained in a limited area with PAT. With respect to imaging, these new nanoparticles gave a clear PA image by themselves, without conjugation with gold, rare earth metals, or dyes. Further studies are currently underway to evaluate the *in vivo* toxicity and biodistribution of the present nanoparticles, and to explore their specific functionalization by antibodies for accumulation in tumors.

ACKNOWLEDGEMENTS

This work was partly supported by the Creation of Innovation Centersfor Advanced Interdisciplinary Research Areas Program "InnovativeTechno-Hub for Integrated Medical Bio-imaging" from the Ministry of Education, Culture, Sports, Science and Technology (MEXT), Japan. YK acknowledges financial support from JSPS KAKENHI Grant Number 25870359, and TK acknowledges financial support from SEI Group CSR Foundation.

REFERENCES

1. Harry VN, Semple SI, Parkin DE, Gilbert FJ. Use of new imaging techniques to predict tumour response to therapy. Lancet Oncol. 2010; 11: 92-102.
2. Jennings LE, Long NJ. 'Two is better than one'--probes for dual-modality molecular imaging. Chem Commun (Camb). 2009; 3511-3524.
3. Louie A. Multimodality imaging probes: design and challenges. Chem Rev. 2010; 110: 3146-3195.
4. Kimura Y, Kamisugi R, Narazaki M, Matsuda T, Tabata Y, Toshimitsu A. Size-controlled and biocompatible Gd_2 O_3 nanoparticles for dual photoacoustic and MR imaging. Adv Healthc Mater. 2012; 1: 657-660.
5. Wang LV, Hu S. Photoacoustic tomography: in vivo imaging from organelles to organs. Science. 2012; 335: 1458-1462.
6. Zackrisson S, van de Ven SM, Gambhir SS. Light in and sound out: emerging translational strategies for photoacoustic imaging. Cancer Res. 2014; 74: 979-1004.

7. Wang Y, Xie X, Wang X, Ku G, Gill KL, O'Neal DP, et al. Photoacoustic tomography of a nanoshell contrast agent in the in vivo rat brain. Nano Lett. 2004; 4: 1689-1692.

8. Song KH, Kim C, Cobley CM, Xia Y, Wang LV. Near-infrared gold nanocages as a new class of tracers for photoacoustic sentinel lymph node mapping on a rat model. Nano Lett. 2009; 9: 183-188.

9. Yang X, Skrabalak SE, Li ZY, Xia Y, Wang LV. Photoacoustic tomography of a rat cerebral cortex in vivo with au nanocages as an optical contrast agent. Nano Lett. 2007; 7: 3798-3802.

10. Agarwal A, Huang SW, O'Donnell M, Day KC, Day M, Kotov N, et al. Targeted gold nanorod contrast agent for prostate cancer detection by photoacoustic imaging. J Appl Phys. 2007; 102: 064701.

11. Eghtedari M, Liopo AV, Copland JA, Oraevsky AA, Motamedi M. Engineering of hetero-functional gold nanorods for the in vivo molecular targeting of breast cancer cells. Nano Lett. 2009; 9: 287-291.

12. Eghtedari M, Oraevsky A, Copland JA, Kotov NA, Conjusteau A, Motamedi M. High sensitivity of in vivo detection of gold nanorods using a laser optoacoustic imaging system. Nano Lett. 2007; 7: 1914-1918.

13. Kim K, Huang S-W, Ashkenazi S, O'Donnell M, Agarwal A, Kotov NA, et al. Photoacoustic imaging of early inflammatory response using gold nanorods. Appl Phys Lett. 2007; 90: 223901.

14. Li C, Wang LV. Photoacoustic tomography and sensing in biomedicine. Phys Med Biol. 2009; 54: R59-97.

15. Song KH, Kim C, Maslov K, Wang LV. Noninvasive in vivo spectroscopic nanorod-contrast photoacoustic mapping of sentinel lymph nodes. Eur J Radiol. 2009; 70: 227-231.

16. Sitharaman B, Kissell KR, Hartman KB, Tran LA, Baikalov A, Rusakova I. Superparamagnetic gadonanotubes are high-performance MRI contrast agents. Chem Commun (Camb). 2005; 3915-3917.

17. Gruber K, Puffer B, Kräutler B. Vitamin B12-derivatives-enzyme cofactors and ligands of proteins and nucleic acids. Chem Soc Rev. 2011; 40: 4346-4363.

18. Bouchard LS, Anwar MS, Liu GL, Hann B, Xie ZH, Gray JW. Picomolar sensitivity MRI and photoacoustic imaging of cobalt nanoparticles. Proc Natl Acad Sci U S A. 2009; 106: 4085-4089.

19. Seo WS, Shim JH, Oh SJ, Lee EK, Hur NH, Park JT. Phase- and size-controlled synthesis of hexagonal and cubic CoO nanocrystals. J Am Chem Soc. 2005; 127: 6188-6189.

20. Kolate A, Baradia D, Patil S, Vhora I, Kore G, Misra A2. PEG - a versatile conjugating ligand for drugs and drug delivery systems. J Control Release. 2014; 192: 67-81.

21. Glaspell GP, Jagodzinski PW, Manivannan A. Formation of cobalt nitrate hydrate, cobalt oxide, and cobalt nanoparticles using laser vaporization controlled condensation. J Phys Chem B. 2004; 108: 9604-9607.

22. Nam KM, Shim JH, Han D-W, Kwon HS, Kang Y-M, Li Y, et al. Syntheses and characterization of wurtzite CoO, rocksalt CoO, and spinel Co_3O_4 nanocrystals: Their interconversion and tuning of phase and morphology. Chem Mater. 2010; 22:4446-4454.

23. Qian Y, Wei P, Jiang P, Li Z, Yan Y, Ji K, et al. Preparation of shape-stabilized co-crystallized poly(ethylene glycol) composites as thermal energy storage materials. Energy Conv Manag. 2013; 76:101-108.

24. Li D, He Q, Zhu H, Tao C, Li J. Enhanced dispersity of gold nanoparticles modified by omega-carboxyl alkanethiols under the impact of poly(ethylene glycol)s. J Nanosci Nanotechnol. 2007; 7: 3089-3094.

Cite this article

Yu Kimura1,2, Takuya Kurimoto2, Yuta Imai,2 Hiro-aki Sugii2, Akio Toshimitsu2, et al. (2014) Novel Biocompatible Cobalt Oxide Nanoparticles for Use in Dual Photoacoustic and Magnetic Resonance Imaging. JSM Biotechnol Bioeng 2(2): 1043.